Vital Surveillances

Variations in the Bacterial Ecosystems of Mosquito Populations — Haikou and Sanya Cities, Hainan Province, China, 2019

Xun Kang[1,2,&]; Yanhong Wang[3,&]; Rui Zheng[1]; Rajaofera Mamy Jayne Nelly[1]; Lin Liu[1]; Siping Li[1]; Xiaomei Sun[3,4]; Le Kang[3,4]; Nan Zhang[1,5,#]; Zhen Zou[4,#]; Qianfeng Xia[1,#]

ABSTRACT

Introduction: This study explores the midgut microbiota of mosquitoes in Haikou and Sanya cities, regions critical for understanding vector-borne disease dynamics in Hainan Province, China. It provides baseline data on microbial composition and examines their potential role in influencing mosquito biology and vector competence, while highlighting the need for further research into their association with vector-borne viral infections.

Methods: Adult mosquitoes were collected using light traps and human bait methods. Species identification was conducted through morphological examination and DNA barcoding using the cytochrome c oxidase subunit 1 gene (cox1). The V3–V4 hypervariable regions of the microbial 16S ribosomal RNA (rRNA) gene were sequenced using high-throughput methods to investigate the midgut microbiota. Statistical analyses, including Alpha and Beta diversity assessments of the sequencing results, were performed using SPSS 21.0 and R version 3.11.

Results: The predominant mosquito species identified were *Aedes albopictus*, *Armigeres subalbatus*, and *Culex pipiens*. Microbiota analysis of 281 midguts revealed that *Proteobacteria* dominated (85.28%), with significant fractions being *Alphaproteobacteria* (52.14%), *Gammaproteobacteria* (29.90%), and *Betaproteobacteria* (3.22%). Other notable phyla included *Firmicutes* (6.24%), *Actinobacteria* (3.81%), and lesser quantities of *Thermi*, *Cyanobacteria*, and *Bacteroidetes*. Significant geographic variation in bacterial communities was observed between Haikou and Sanya (P<0.05), with unique taxa like *Thermi* and *Cyanobacteria* identified only in Haikou and *Chlamydiae* found solely in Sanya. The analysis revealed 204 overlapping species, with 473 unique to Haikou and 64 to Sanya.

Conclusions: This study revealed significant geographic differences in the midgut microbiota of mosquitoes from Haikou and Sanya, providing foundational data for understanding their potential impact on mosquito biology and disease transmission. While the direct relationship between these microbial variations and vector-borne disease dynamics requires further investigation, these findings underscore the importance of mosquito microbiota research as part of broader strategies to mitigate vector-borne disease risks.

Mosquitoes serve as crucial vectors for infectious diseases such as Zika and dengue, particularly affecting tropical regions like Hainan Province, China (*1*). With over 3,500 species worldwide, mosquitoes play significant roles in both public health and ecosystem dynamics (*2*). Their blood-feeding behavior directly connects them to vertebrate hosts, making them primary carriers of various pathogens (*3*). The midgut of female mosquitoes functions as a key site for both pathogen entry and blood digestion, hosting diverse microbial communities that influence disease transmission capacity (*4*). This microbiota can significantly affect mosquito development and pathogen resistance, highlighting its importance in contemporary entomological research.

Symbiotic relationships between organisms and their microbiomes are well-established phenomena that influence various biological processes. In female mosquitoes, particularly those that feed on blood, the midgut serves as both a digestion site and an entry point for pathogens including viruses, protozoa, and nematodes (*5*–*6*). Research has demonstrated that the microbiome within the midgut significantly influences vector competence — the ability to acquire, maintain, and transmit pathogens to vertebrates (*7*). Additionally, gut bacteria affect the biological development of mosquitoes and can modulate their vulnerability to pathogens. Increased diversity and abundance of gut bacteria have been linked to reduced

susceptibility to pathogens, suggesting potential disease control strategies (*8*).

In Hainan, the tropical monsoon climate and extensive forest coverage provide an ideal environment for mosquito proliferation. A recent surge in dengue cases underscores the need for enhanced understanding of mosquito microbiomes to develop novel disease control strategies (*9*). Our study examines the midgut microbiota of mosquitoes from Haikou and Sanya cities, exploring how environmental factors shape microbial diversity and influence disease transmission potential. This research contributes to both our understanding of mosquito-borne disease dynamics and ongoing efforts to control these diseases through targeted microbial interventions.

METHODS

Mosquito Collection

Adult female mosquitoes were collected over an eight-day period (July 12–19, 2019) in Haikou and Sanya cities, Hainan Province, China. Collection sites were selected in tropical and subtropical areas using CO_2-augmented light traps and human landing catches to ensure diverse sampling (*10*). The collection sites and their geographic coordinates are presented in Table 1.

Identification and Processing

Mosquitoes were identified morphologically, and their identities were confirmed via DNA barcoding using the cytochrome c oxidase subunit 1 (cox1) gene (*11*). All specimens were stored at −80 °C. To minimize the influence of host blood on microbiota analysis, blood-fed mosquitoes were maintained in the laboratory for 4 days to allow for blood digestion before midgut dissection.

DNA Extraction

Following molecular identification, mosquitoes were sorted by species, and ten midguts per species were dissected in triplicate to ensure data reliability. The samples were initially stored at −80 °C, surface-sterilized in 75% ethanol for 30 seconds, and this process was repeated twice. After rinsing twice in sterile PBS to remove residual ethanol, the midguts were pooled into sterile 1.5 mL tubes and stored at −20 °C until DNA extraction (*12*). Dissections were performed under a stereomicroscope to ensure sample integrity, with the foregut, hindgut, and Malpighian tubules carefully removed. Genomic DNA was extracted using the DNeasy Blood & Tissue Kit (Qiagen, USA) (*13*) according to the manufacturer's instructions. The purified DNA was diluted in 50 µL ddH_2O for microbiome library construction at BGI Shenzhen.

16S rRNA Gene Library Preparation, Illumina HiSeq Sequencing

A total of 281 midguts were collected from various mosquito species in Haikou and Sanya, using primers 338F (5'-ACTCCTACGGGAGGCAGCA-3') and 806R (5'-GGACTACHVGGGTWTCTAAT-3') to amplify the V3-V4 hypervariable regions of the bacterial 16S rRNA gene (*14*). The genomic DNA was sequenced using the Illumina HiSeq 4000 system.

TABLE 1. Geographic coordinates and number of mosquito samples processed for midgut bacteria.

Site	Villages /towns	Geographic coordinates	Mosquito species	Number of midgut samples	
				Initial	Final
Haikou (HK)	Xiyi (XY)	110°19'52.284"E 20°1'55.095"N	*Culex pipiens* (CPI)	42	30
			Culex gelidus (CGE)	13	11
	Xinghui (XH)	110°20'30.01"E 20°02'44.99"N	*Aedes albopictus* (AAL)	35	30
			Culex pipiens (CPI)	34	30
	Changwang (CW)	110°18'17.93"E 20°01'37.16"N.	*Aedes albopictus* (AAL)	35	30
Sanya (SY)	Shiwaitaoyuan (SW)	110°27'31.36"E 19°48'08.82"N	*Armigeres subalbatus* (ASU)	32	30
	Sanya (SY)	109°30'35.96"E 18°15'19.19"N	*Aedes albopictus* (AAL)	34	30
	Nanya (NY)	109°14'25.76"E 18°27'50.47"N	*Armigeres subalbatus* (ASU)	30	30
	Nanbin (NB)	109°11'56.00"E 18°21'37.15"N	*Aedes albopictus* (AAL)	35	30
	Chicao (CC)	109°10'4.51"E 18°24'47.56"N	*Aedes albopictus* (AAL)	34	30
				324	281

Following sequencing, we implemented quality control measures, including the removal of chimeric sequences, and identified Operational Taxonomic Units (OTUs) using the RDP Classifier (*15*). From 1,508,554 raw reads, 1,384,001 clean reads were generated (Supplementary Table S1, available athttps://weekly.chinacdc.cn/) and clustered into OTUs at 97% similarity. Only OTUs with a relative abundance above 0.5% were analyzed to focus on the predominant bacterial communities (Supplementary Table S2, available at https://weekly.chinacdc.cn/).

Statistical Analysis

Statistical evaluations were conducted using R (version 3.1.1; R Foundation, Austria) and Metastats (version 1.0; Whitehead Institute, USA) to assess differentiation among microbial communities (*16*). Rarefaction curves and box plots were generated to visualize biodiversity and analyze significant differences in microbial diversity.

Alpha and Beta Diversity Analyses

Microbial diversity within and across mosquito samples were quantified using alpha and beta diversity indices. Alpha diversity, which measures diversity within a sample, included indices such as Simpson, Shannon, ACE, and Chao1, calculated using Mothur (version 1.31.2; Michigan State University, USA) at a 97% similarity threshold for OTUs. Beta diversity, which compares differences between samples, was evaluated using Bray-Curtis, weighted UniFrac, and unweighted UniFrac indices. Significant differences in *alpha* diversity were observed between mosquito populations in Haikou and Sanya, as visualized by matrix heatmaps of diversity metrics, highlighting the presence, abundance, and phylogenetic relationships of microbial communities.

Visualization and Phylogenetic Analysis

Venn diagrams were used to illustrate shared and unique OTUs, effectively visualizing microbial overlap and distinctiveness across samples. For phylogenetic analysis, sequences were aligned using QIIME's align_seqs.py, and phylogenetic trees were constructed using the Fasttree method (*17*). These trees, representing evolutionary relationships among bacterial *species*, were visualized using R software, providing comprehensive insights into the microbial community structure across different environmental contexts.

Cluster Analysis Methodology

Cluster analysis was performed using QIIME (version 1.8.0; Knight Lab, University of Colorado, USA) with an iterative algorithm that selected 75% of sequence data from the least abundant samples. The Unweighted Pair Group Method with Arithmetic Mean (UPGMA) was employed for hierarchical clustering to reveal relationships among microbial communities. The resulting clustering trees were visualized using R software, effectively illustrating the structural organization of microbial communities across the studied samples (*18*).

RESULTS

Mosquito Microbial Community Composition

This study analyzed the V3–V4 regions of the 16S rRNA gene in 281 midguts from field-collected female mosquitoes (*Aedes albopictus*, *Culex pipiens*, *Culex gelidus*, and *Armigeres subalbatus*) from Haikou and Sanya. The majority of sequences belonged to the *phylum Proteobacteria* (85.28%), primarily *Alphaproteobacteria* (52.14%), *Gammaproteobacteria* (29.90%), and *Betaproteobacteria* (3.22%). Other significant *phyla* included *Firmicutes* (6.24%), *Actinobacteria* (3.81%), and smaller contributions from *Thermi*, *Cyanobacteria*, *Bacteroidetes*, *Spirochaetes*, *TM7*, and *Chloroflexi*. At the *family* level, *Rickettsiaceae* dominated (46.96%), followed by *Enterobacteriaceae* and *Aeromonadaceae*. The most abundant *genera* were *Wolbachia* (46.96%), *Acinetobacter*, and *Escherichia* (Figure 1A–B). *Rickettsiaceae* prevalence varied by location, being higher in Sanya (87.36% in *Ae. albopictus* and *Ar. subalbatus*) compared to Haikou (20.02%), with a much lower abundance in *Ae. albopictus* from XH (0.32%). This demonstrates significant variations in the gut microbiomes across mosquito species and different locations.

Venn Analysis of Midgut Bacteria

OTUs were defined at 97% similarity, and shared an unique taxa were visualized with Venn diagrams to identify core microorganisms across environments. Comparative analysis revealed that mosquito species within the same *genus* in Haikou and Sanya harbored similar bacteria, with 204 overlapping *species*, 473 unique *species* in Haikou, and 64 unique *species* in Sanya (Figure 2A). *Phylum*-level analysis showed distinct bacterial communities between the two

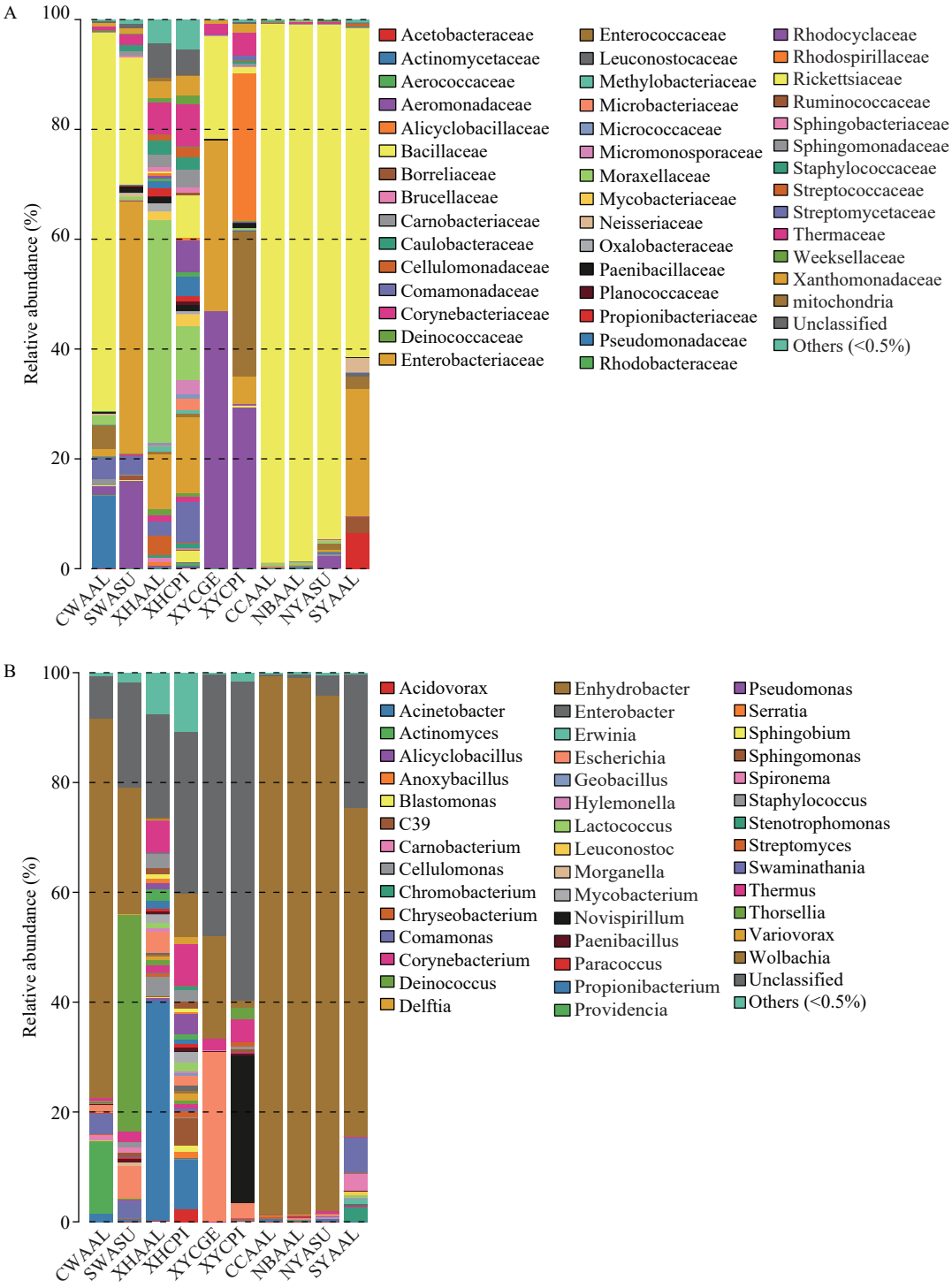

FIGURE 1. Mean relative abundances of (A) bacterial families and (B) genera associated with four mosquito species from Haikou and Sanya.
Note: Families and genera with abundance less than 0.5% were pooled together as "Other."
Abbreviation: CW=Changwang, HK; SW=Shiwaitaoyuan, HK; XH=Xinghui, HK; XY=Xiyi, HK; CC=Chicao, SY; HK=Haikou; NB=Nanbin, SY; NY=Nanya, SY; SY=Sanya; AAL=*Aedes albopictus*, ASU=*Armigeres subalbatus*, CGE=*Culex gelidus*, CPI=*Culex pipiens*.

locations. Haikou was dominated by *Firmicutes* (32.77%), followed by *Proteobacteria* (23.26%), and *Bacteroidetes* (16.28%), while Sanya had higher proportions of *Proteobacteria* (32.81%) and *Firmicutes*

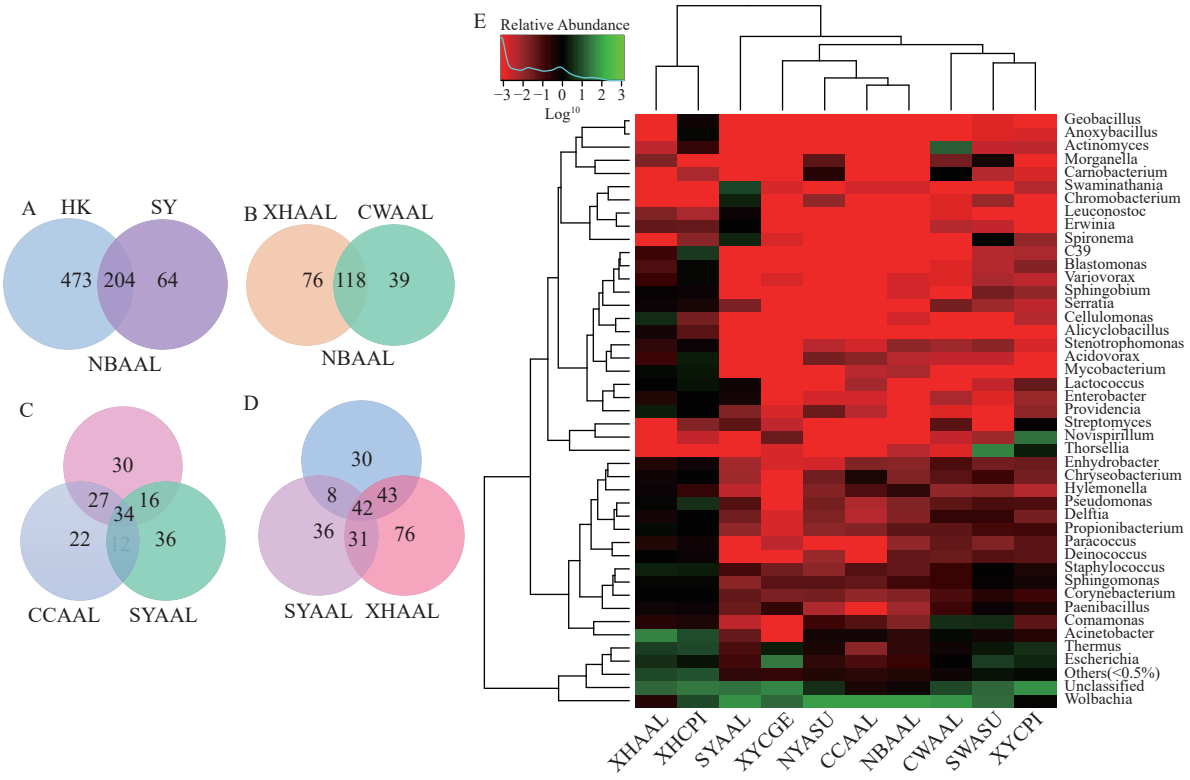

FIGURE 2. Venn diagrams and heatmap illustrating bacterial composition overlap and gut microbiota of mosquito species across habitats. (A) Venn diagram showing overlaps of OTUs at 97% similarity between the HK and SY data sets; (B) Number of bacterial taxa specific and common to *Aedes albopictus* of XH, CW in Haikou; (C) Number of bacterial taxa specific and common to *Ae. albopictus* of CC, NB, SY (street) in Sanya; (D) Number of bacterial taxa specific and common to *Aedes albopictus* of XH, NB, and SY; (E) Heatmap in log scale depicting the gut bacterial community of mosquito midguts obtained with open reference OTU picking methods at the *genus* level.
Note: For (E), Green colors represent high abundance, and red colors represent low abundance; black indicates absence.
Abbreviation: OTUs=Operational Taxonomic Units; CW=Changwang, HK; SW=Shiwaitaoyuan, HK; XH=Xinghui, HK; XY=Xiyi, HK; CC=Chicao, SY; HK=Haikou; NB=Nanbin, SY; NY=Nanya, SY; SY=Sanya.

(26.56%). Haikou also contained unique phyla, including *Thermi* and *Cyanobacteria*, while Sanya exclusively harbored *Chlamydiae*. Statistical tests confirmed significant differences between locations, such as for *Actinobacteria* (Wilcoxon test: P=0.038).

Further analysis of *Ae. albopictus* in Haikou revealed that XH and CW shared 118 species, with 76 and 39 unique species, respectively, indicating greater diversity in XH (Figure 2B). In contrast, three Sanya locations (SY, CC, NB) shared only 34 species, demonstrating lower diversity (Figure 2C). Between Haikou's XH and Sanya's SY and NB, 42 overlapping species were found (Figure 2D), with fewer unique species in Nanban farm and Sanya Street (30 and 36, respectively) compared to Haikou's Xinghui Village (76 unique *species*). Across all sites, 32 *species* were consistently identified, representing a core microbial community. Key *genera* included *Corynebacterium*, *Wolbachia* and *Cupriavidus*.

Analysis of *species* and Their Abundance

The phylogenetic tree and heatmap visually represent the composition and abundance of bacterial communities in mosquito midguts, highlighting structural similarities and differences. Clustering analyses revealed three major groups: 1) *Ae. albopictus* and *Cx. pipiens* from XH Village in Haikou; 2) *Cx. gelidus* from XY Village, along with *Ae. albopictus* from NY Farm, CC Village, and Sanya Street; and 3) mosquitoes from CW, SW, and XY Villages in Haikou. Three primary *genera* were identified: *Wolbachia*, *Escherichia*, and *Thermus*, which were widespread across locations and species. *Wolbachia* was abundant in all mosquitoes except for those from XH and XY Villages. *Acinetobacter* and *Comamonas* were found predominantly in *Ae. albopictus* and *Cx. pipiens* from XH Village and *Ae. albopictus* and *Ar. subalbatus* from CW and SW Villages. *Novispirillum* and *Thorsellia* were more abundant in *Cx. pipiens* from XY

Village and *Ar. subalbatus* from SW Village (Figure 2E).

The Diversity Analysis of Intestinal Bacteria in Regions

Alpha diversity indices (observed *species*, Chao1, ACE, Simpson, and Shannon) were used to assess bacterial diversity and richness in mosquitoes from Haikou and Sanya, revealing differences between locations. Alpha diversity showed significantly higher bacterial richness in *Cx. pipiens* from Haikou compared to *Ae. albopictus* from Sanya, with *Cx. pipiens* and *Ar. subalbatus* in Haikou exhibiting notably higher diversity (Chao1: 491.54, ACE: 487.92; Chao1: 411.25, ACE: 405.33) versus Sanya (Chao1: 220.87, ACE: 261.89) (Figure 3A).

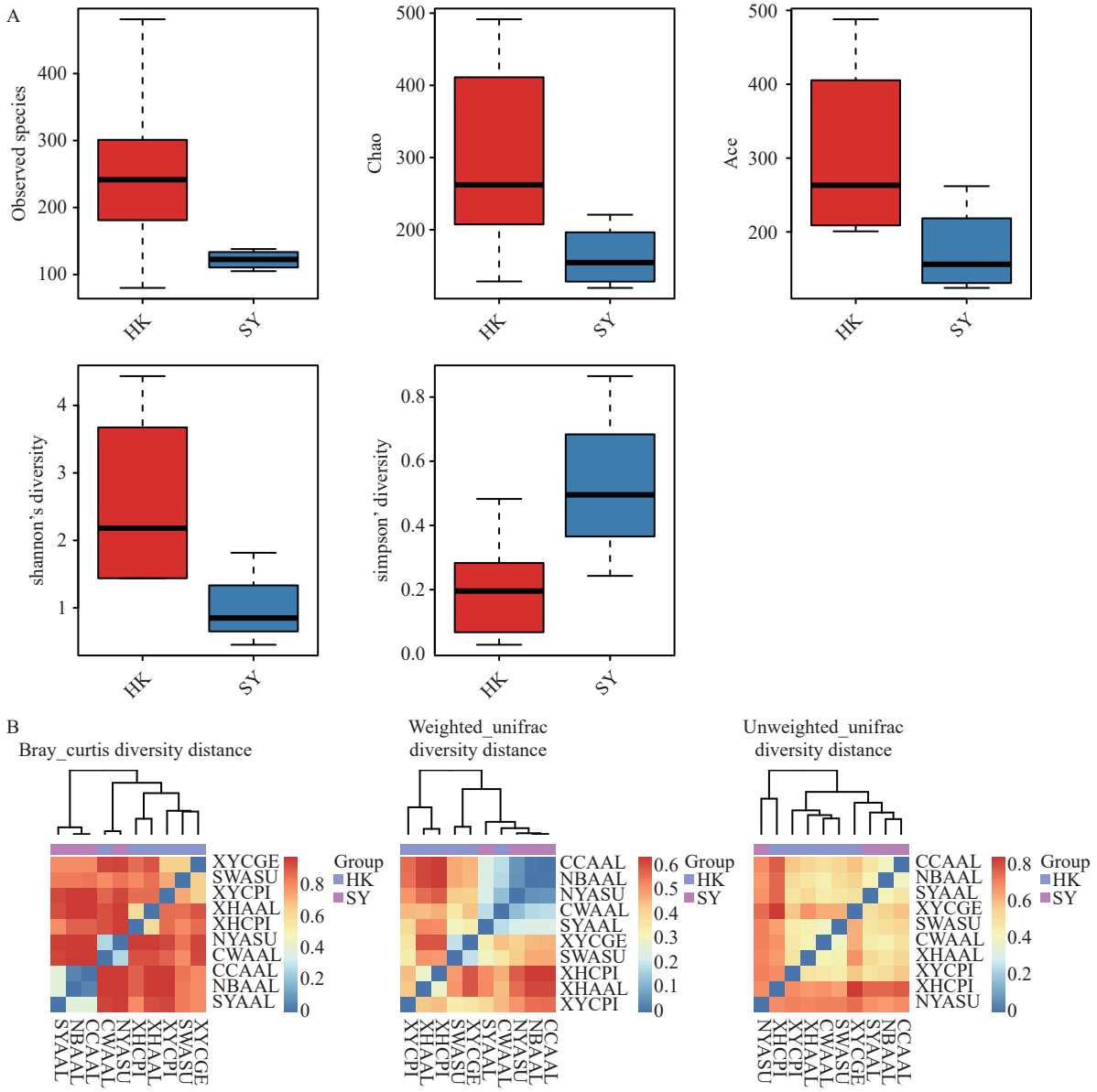

FIGURE 3. Boxplot and heatmap representations of bacterial diversity across mosquito species and habitats. (A) Boxplot representation of observed *species*, Chao1, and Shannon diversity indices. (B) Matrix heatmap of Bray-Curtis distances (left), Weighted UniFrac Beta diversity (middle), and Unweighted UniFrac Beta diversity (right) between microbial communities of four mosquito species from Haikou and Sanya.

Note: For (A), boxplots show the distribution of bacteria between mosquito samples categorized by location and species. Significant differences between the groups were investigated using pairwise comparisons of means (Dunn test; *P* value adjustment: Holm). *Species* richness is represented by the number of bands. Boxplots show median, minimum, and maximum values, with black lines indicating medians.

Beta diversity analysis revealed significant microbial differences between Haikou and Sanya populations, with Bray-Curtis, weighted UniFrac, and unweighted UniFrac metrics demonstrating distinct clustering patterns (Figure 3B). Bray-Curtis indicated dissimilarity between *Ar. subalbatus* (SY-ASU) from Sanya and *Cx. gelidus* (HK-CGE) and *Ae. albopictus* (HK-AAL) from Haikou, while *Ae. albopictus* from both regions overlapped. The unweighted UniFrac distance metric highlighted the microbial divergence between *Cx. gelidus* (HK-CGE) and *Ar. subalbatus* (SY-ASU), while *Ae. albopictus* populations showed greater similarity. The weighted UniFrac metric revealed microbial overlap between *Ae. albopictus* (SY-AAL) and *Ar. subalbatus* (SY-ASU) in Sanya, but distinctions from *Cx. pipiens* (HK-CPI) and *Cx. gelidus* (HK-CGE) in Haikou. These patterns indicate that microbial communities in Sanya were more similar within the region, while those in Haikou exhibited more variation. Overall, geographic and species-specific factors strongly influence microbial community composition.

CONCLUSIONS

This study investigated bacterial communities in the midguts of four mosquito species from Haikou and Sanya using high-throughput sequencing of the 16S rRNA gene's V3-V4 regions. *Proteobacteria*, particularly *Wolbachia*, dominated the microbial composition, with significantly higher prevalence in Sanya than in Haikou, suggesting regional differences in microbial composition that could influence disease transmission dynamics (*19*).

Blood meals substantially alter gut microbiota, increasing bacteria such as *Serratia* and *Elizabethkingia* that participate in blood digestion, while reducing symbiotic bacteria like *Wolbachia*, which may affect mosquito immunity and vector competence (*20*). To minimize blood-feeding effects, mosquitoes were allowed to digest blood for 4 days before dissection, though residual effects on bacterial diversity cannot be ruled out. Regional and species-specific variations, such as the higher prevalence of *Wolbachia* in Sanya mosquitoes, may also be influenced by dietary and environmental factors. Future studies should include controlled feeding experiments to distinguish intrinsic microbiota from transient changes due to blood meals.

Venn diagrams revealed both shared and unique microbial communities between locations. Mosquitoes from Haikou displayed richer bacterial diversity, including *Thermi* and *Cyanobacteria*, indicating regional variations. Alpha diversity was higher *Cx. pipiens* from Haikou than in *Ae. albopictus* from Sanya, highlighting the importance of understanding local mosquito ecology for disease control. Phylogenetic and heatmap analyses showed distinct microbial clusters based on geographic location and mosquito species, reflecting the complex interplay between mosquitoes and their microbiomes and suggesting the influence of environmental factors. However, the analysis was limited to four mosquito species and two regions, and 16S rRNA sequencing offers limited taxonomic resolution.

In conclusion, significant variations in microbial ecosystems were found between mosquito populations from Haikou and Sanya, with *Wolbachia*'s higher prevalence in Sanya mosquitoes, indicating potential for biologically-based control strategies to enhance public health in tropical regions (*21*).

Conflicts of interest: No conflicts of interest.

Funding: Supported by the Hainan Provincial Natural Science Foundation of China (824QN269, 822QN324), Hainan Province Science and Technology Talent Innovation Project (KJRC2023D29), Hainan Tropical Disease Research Center (Hainan Sub-Center, Chinese Center for Tropical Disease Research) (HNTDC202303), National Key Plan for Scientific Research and Development of China (2023YFA1801002).

doi: 10.46234/ccdcw2025.086

[#] Corresponding authors: Qianfeng Xia, xiaqianfeng@hainmc.edc.cn; Zhen Zou, zouzhen@ioz.ac.cn; Nan Zhang, hy0211075@hainmc.edu.cn.

[1] NHC Key Laboratory of Tropical Disease Control, School of Tropical Medicine, Hainan Medical University, Haikou City, Hainan Province, China; [2] Hainan Tropical Disease Research Center (Hainan Sub-Center, Chinese Center for Tropical Disease Research), Haikou City, Hainan Province, China; [3] State Key Laboratory of Integrated Management of Pest Insects and Rodents, Institute of Zoology, Chinese Academy of Sciences, Beijing, China;; [4] CAS Center for Excellence in Biotic Interactions, University of Chinese Academy of Sciences, Beijing, China; [5] School of Biomedical Engineering, Sun Yat-sen University, Shenzhen City, Guangdong Province, China.
[&] Joint first authors.

Submitted: June 13, 2024
Accepted: April 13, 2025
Issued: April 18, 2025

REFERENCES

1. Liu L, Wu T, Liu B, Nelly RMJ, Fu YM, Kang X, et al. The origin and

molecular epidemiology of dengue fever in Hainan Province, China, 2019. Front Microbiol 2021;12:657966. https://doi.org/10.3389/fmicb.2021.657966.
2. De Niz M, Kehrer J, Brancucci NMB, Moalli F, Reynaud EG, Stein JV, et al. 3D imaging of undissected optically cleared *Anopheles stephensi* mosquitoes and midguts infected with *Plasmodium parasites*. PLoS One 2020;15(9):e0238134. https://doi.org/10.1371/journal.pone.0238134.
3. Coon KL, Valzania L, McKinney DA, Vogel KJ, Brown MR, Strand MR. Bacteria-mediated hypoxia functions as a signal for mosquito development. Proc Natl Acad Sci USA 2017;114(27):E5362 – 9. https://doi.org/10.1073/pnas.1702983114.
4. Michalski ML, Erickson SM, Bartholomay LC, Christensen BM. Midgut barrier imparts selective resistance to filarial worm infection in *Culex pipiens pipiens*. PLoS Negl Trop Dis 2010;4(11):e875. https://doi.org/10.1371/journal.pntd.0000875.
5. Sun XM, Wang YH, Yuan F, Zhang YA, Kang X, Sun J, et al. Gut symbiont-derived sphingosine modulates vector competence in *Aedes* mosquitoes. Nat Commun 2024;15(1):8221. http://dx.doi.org/10.1038/s41467-024-52566-1.
6. Dada N, Jupatanakul N, Minard G, Short SM, Akorli J, Villegas LM. Considerations for mosquito microbiome research from the Mosquito Microbiome Consortium. Microbiome 2021;9(1):36. https://doi.org/10.1186/s40168-020-00987-7.
7. Muturi EJ, Bara JJ, Rooney AP, Hansen AK. Midgut fungal and bacterial microbiota of *Aedes triseriatus* and *Aedes japonicus* shift in response to La Crosse virus infection. Mol Ecol 2016;25(16):4075 – 90. https://doi.org/10.1111/mec.13741.
8. Coatsworth H, Caicedo PA, Van Rossum T, Ocampo CB, Lowenberger C. The composition of midgut bacteria in *Aedes aegypti* (diptera: culicidae) that are naturally susceptible or refractory to dengue viruses. J Insect Sci 2018;18(6):12. https://doi.org/10.1093/jisesa/iey118.
9. Liu Q, Cui F, Liu X, Fu YM, Fang WJ, Kang X, et al. Association of virome dynamics with mosquito species and environmental factors. Microbiome 2023;11(1):101. https://doi.org/10.1186/s40168-023-01556-4.
10. Kang X, Wang YH, Li SP, Sun XM, Lu XY, Rajaofera MJN, et al. Comparative analysis of the gut microbiota of adult mosquitoes from eight locations in Hainan, China. Front Cell Infect Microbiol 2020;10:596750. https://doi.org/10.3389/fcimb.2020.596750.
11. Wilke ABB, de Oliveira Christe R, Multini LC, Vidal PO, Wilk-da-Silva R, de Carvalho GC, et al. Morphometric wing characters as a tool for mosquito identification. PLoS One 2016;11(8):e0161643. https://doi.org/10.1371/journal.pone.0161643.
12. Tutagata J, Pocquet N, Trouche B, Reveillaud J. Dissection of mosquito ovaries, midgut, and salivary glands for microbiome analyses at the organ level. J Vis Exp 2024;000(212):13. http://dx.doi.org/10.3791/67128.
13. Yadav KK, Bora A, Datta S, Chandel K, Gogoi HK, Prasad GBKS, et al. Molecular characterization of midgut microbiota of *Aedes albopictus* and *Aedes aegypti* from Arunachal Pradesh, India. Parasit Vectors 2015;8:641. https://doi.org/10.1186/s13071-015-1252-0.
14. Zhang JH, Yu N, Xu XX, Liu ZW. Community structure, dispersal ability and functional profiling of microbiome existing in fat body and ovary of the brown planthopper, *Nilaparvata lugens*. Insect Sci 2019;26(4):683 – 694. https://doi.org/10.1111/1744-7917.12575.
15. Wang Y, Gilbreath III TM, Kukutla P, Yan GY, Xu JN. Dynamic gut microbiome across life history of the malaria mosquito *Anopheles gambiae* in Kenya. PLoS One 2011;6(9):e24767. https://doi.org/10.1371/journal.pone.0024767.
16. Huber W, Carey VJ, Gentleman R, Anders S, Carlson M, Carvalho BS, et al. Orchestrating high-throughput genomic analysis with Bioconductor. Nat Methods 2015;12(2):115 – 21. https://doi.org/10.1038/nmeth.3252.
17. Caporaso JG, Kuczynski J, Stombaugh J, Bittinger K, Bushman FD, Costello EK, et al. QIIME allows analysis of high-throughput community sequencing data. Nat Methods 2010;7(5):335 – 6. https://doi.org/10.1038/nmeth.f.303.
18. Schloss PD, Westcott SL, Ryabin T, Hall JR, Hartmann M, Hollister EB, et al. Introducing mothur: open-source, platform-independent, community-supported software for describing and comparing microbial communities. Appl Environ Microbiol 2009;75(23):7537 – 41. https://doi.org/10.1128/AEM.01541-09.
19. Hugo LE, Stassen L, La J, Gosden E, Ekwudu O, Winterford C, et al. Vector competence of Australian *Aedes aegypti* and *Aedes albopictus* for an epidemic strain of Zika virus. PLoS Negl Trop Dis 2019;13(4):e0007281. https://doi.org/10.1371/journal.pntd.0007281.
20. Flores GAM, Lopez RP, Cerrudo CS, Perotti MA, Consolo VF, Berón CM. *Wolbachia dominance* influences the *Culex quinquefasciatus* microbiota. Sci Rep 2023;13(1):18980. https://doi.org/10.1038/s41598-023-46067-2.
21. Monteiro VVS, Navegantes-Lima KC, de Lemos AB, da Silva GL, de Souza Gomes R, Reis JF, et al. *Aedes*-chikungunya virus interaction: key role of vector midguts microbiota and its saliva in the host infection. Front Microbiol 2019;10:492. https://doi.org/10.3389/fmicb.2019.00492.

SUPPLEMENTARY MATERIAL

SUPPLEMENTARY TABLE S1. Total of raw reads and clean reads (Mean±SE) of mosquito samples in Haikou and Sanya.

Total group name	Sample name	Raw reads	Clean reads
HK-AAL	CWAAL1	70,891	68,031
	CWAAL2	72,279	63,213
	XHAAL	35,568	28,714
HK-CPI	XYCPI1	56,087	52,400
	XYCPI2	72,649	68,035
	XYCPI3	75,244	67,931
	XHCPI1	35,283	32,180
	XHCPI2	51,493	47,317
	XHCPI3	35,079	28,335
HK-ASU	SWASU1	73,236	68,226
	SWASU2	72,354	66,109
	SWASU3	72,157	66,638
HK-CGE	XYCGE	72,319	67,306
SY-AAL	NBAAL1	56,890	52,681
	NBAAL2	57,483	52,904
	NBAAL3	55,997	52,694
	CCAAL1	57,124	53,717
	CCAAL2	57,182	53,787
	CCAAL3	57,690	53,796
	SYAAL1	67,396	62,515
	SYAAL2	59,038	55,249
	SYAAL3	68,797	61,006
SY-ASU	NYASU1	58,182	53,889
	NYASU2	59,052	53,825
	NYASU3	59,084	53,503
Sum		1,508,554	1,384,001
Mean		60,342.16	55,360.04
SE		11,652.34	11,422.78

SUPPLEMENTARY TABLE S2. Sequences from mosquitoes in Haikou and Sanya were clustered into 21 bacterial OTUs belonging to 21 *phyla*, 45 *families*, and 45 *genera*. Filtered tags were clustered into OUT with 97% similarity.

#OTUId Abundance	*Phylum*	*Families*	*Genera*
Otu787	*Acidobacteria*	*Acetobacteraceae*	*Acidovorax*
Otu306	*Actinobacteria*	*Actinomycetaceae*	*Acinetobacter*
Otu161	*Armatimonadetes*	*Aerococcaceae*	*Actinomyces*
Otu77	*Bacteroidetes*	*Aeromonadaceae*	*Alicyclobacillus*
Otu46	*Chlamydiae*	*Alicyclobacillaceae*	*Anoxybacillus*
Otu45	*Chloroflexi*	*Bacillaceae*	*Blastomonas*
Otu56	*Cyanobacteria*	*Borreliaceae*	*C39*
Otu229	*Fibrobacteres*	*Brucellaceae*	*Carnobacterium*
Otu80	*Firmicutes*	*Carnobacteriaceae*	*Cellulomonas*
Otu86	*Fusobacteria*	*Caulobacteraceae*	*Chromobacterium*
Otu8	*GN02*	*Cellulomonadaceae*	*Chryseobacterium*
Otu7	*Gemmatimonadetes*	*Comamonadaceae*	*Comamonas*
Otu99	*Planctomycetes*	*Corynebacteriaceae*	*Corynebacterium*
Otu105	*Proteobacteria*	*Deinococcaceae*	*Deinococcus*
Otu133	*Spirochaetes*	*Enterobacteriaceae*	*Delftia*
Otu28	*TM7*	*Enterococcaceae*	*Enhydrobacter*
Otu26	*Tenericutes*	*Leuconostocaceae*	*Enterobacter*
Otu20	*Thermi*	*Methylobacteriaceae*	*Erwinia*
Otu37	*Thermotogae*	*Microbacteriaceae*	*Escherichia*
Otu15	Unclassified	*Micrococcaceae*	*Geobacillus*
Otu12	*Verrucomicrobia*	*Micromonosporaceae*	*Hylemonella*
		Moraxellaceae	*Lactococcus*
		Mycobacteriaceae	*Leuconostoc*
		Neisseriaceae	*Morganella*
		Oxalobacteraceae	*Mycobacterium*
		Paenibacillaceae	*Novispirillum*
		Planococcaceae	*Paenibacillus*
		Propionibacteriaceae	*Paracoccus*
		Pseudomonadaceae	*Propionibacterium*
		Rhodobacteraceae	*Providencia*
		Rhodocyclaceae	*Pseudomonas*
		Rhodospirillaceae	*Serratia*
		Rickettsiaceae	*Sphingobium*
		Ruminococcaceae	*Sphingomonas*
		Sphingobacteriaceae	*Spironema*
		Sphingomonadaceae	*Staphylococcus*
		Staphylococcaceae	*Stenotrophomonas*
		Streptococcaceae	*Streptomyces*
		Streptomycetaceae	*Swaminathania*
		Thermaceae	*Thermus*
		Unclassified	*Thorsellia*
		Weeksellaceae	Unclassified
		Xanthomonadaceae	*Variovorax*
		mitochondria	*Wolbachia*
		Acetobacteraceae	Others (<0.5%)